Research Article

Received: 13 May 2024 Revised: 19 June 2024 Published online in Wiley Online Library: 28 July 2024

(wileyonlinelibrary.com) DOI 10.1002/jsfa.13770

Unlocking the nutraceutical potential of *Corylus avellana* L. shells: microwave-assisted extraction of phytochemicals with antiradical and anti-diabetic properties

Anna E. Maccarronello,[a] Nunzio Cardullo,[a] Ana Margarida Silva,[b] Antonella Di Francesco,[a] Paulo C. Costa,[c,d] Francisca Rodrigues[b*] and Vera Muccilli[a*]

Abstract

BACKGROUND: In recent years, the demand for high-quality natural extracts to be included in nutraceutical formulations has increased sharply. Hazelnut (*Corylus avellana* L.) shells (HZS) are underrated agricultural by-products that could be exploited as a source of active ingredients with pro-healthy properties. In the present study, a fully green microwave-assisted extraction (MAE) method was established for the first time aiming to recover bioactive constituents from HZS with significant nutraceutical value. Key MAE parameters, including ethanol in water concentration, microwave power, irradiation time and solvent-to-powder ratio, were optimized through response surface methodology utilizing a Box–Behnken design to achieve the highest total phenolic content and antioxidant/antiradical activities in the final extract.

RESULTS: The optimal MAE conditions (28% *v/v* ethanol/water, 270 *s*, 670 *W*, and 37 mL g^{-1}) yielded an extract with significant scavenging capacity against reactive oxygen species and remarkable inhibitory activity towards both α-amylase (IC_{50} = 7.73 μg mL^{-1}) and α-glucosidase (IC_{50} = 49.44 μg mL^{-1}), demonstrating stronger hypoglycaemic properties than the anti-diabetic drug acarbose. Additionally, fluorescence spectroscopy results highlighted the ability of the optimized extract from HZS (OHS-E) to counteract advanced glycation end-product formation throughout the glycation cascade in a dose-dependent manner. Liquid chromatography/electrospray ionization-tandem mass spectrometry profiling unveiled the presence of fatty acids and phenolic compounds, including lignans, flavonoids, gallic acid derivatives and diarylheptanoids. Lastly, the biocompatibility of OHS-E was attested on HT29-MTX and Caco-2 intestinal cells.

CONCLUSION: Altogether, these findings encourage the potential application of OHS-E as an effective nutraceutical component against type 2 diabetes mellitus and oxidative stress.
© 2024 The Author(s). *Journal of the Science of Food and Agriculture* published by John Wiley & Sons Ltd on behalf of Society of Chemical Industry.

Supporting information may be found in the online version of this article.

Keywords: microwave-assisted extraction; response surface methodology; α-glucosidase inhibition; α-amylase inhibition; advanced glycation end-products

INTRODUCTION

Type 2 diabetes mellitus (T2DM) is a globally prevalent pathological condition. One of its primary indicators is postprandial hyperglycaemia, which is typically interconnected with a series of etiological factors, including visceral adiposity, oxidative stress and insulin resistance.[1] Moreover, the tissue accumulation of advanced glycation end products (AGEs), such as glycated haemoglobin (HbA1c), deriving from the non-enzymatic reactions among reducing sugars and free amino groups of peptides, can alter the structure and function of nucleic acids and proteins,

* *Correspondence to: F Rodrigues, REQUIMTE/LAQV, ISEP, Polytechnic of Porto, Rua Dr. António Bernardino de Almeida, 4249-015 Porto, Portugal. E-mail: francisca.rodrigues@graq.isep.ipp.pt; or V Muccilli, Department of Chemical Sciences, University of Catania, V. le A. Doria 6, 95125 Catania, Italy. E-mail: v.muccilli@unict.it*

a *Department of Chemical Sciences, University of Catania, Catania, Italy*

b *REQUIMTE/LAQV, ISEP, Polytechnic of Porto, Porto, Portugal*

c *UCIBIO – Applied Molecular Biosciences Unit, MedTech-Laboratory of Pharmaceutical Technology, Faculty of Pharmacy, University of Porto, Porto, Portugal*

d *Associate Laboratory i4HB – Institute for Health and Bioeconomy, Faculty of Pharmacy, University of Porto, Porto, Portugal*

© 2024 The Author(s). *Journal of the Science of Food and Agriculture* published by John Wiley & Sons Ltd on behalf of Society of Chemical Industry. This is an open access article under the terms of the Creative Commons Attribution License, which permits use, distribution and reproduction in any medium, provided the original work is properly cited.

contributing to inflammation, ageing and T2DM complications, mainly vasculopathy and retinopathies.[2] Although α-amylase and α-glucosidase inhibitors (e.g. acarbose or miglitol), as well as AGE inhibitors (e.g. aminoguanidine (AG)), are typically included in standard T2DM therapeutic protocols, their administration is accompanied by adverse gastrointestinal effects, flu-like symptoms and skin reactions,[3] limiting their tolerability and compliance. Phytochemicals, especially phenolic compounds, have been suggested to be effective in scavenging reactive oxygen species (ROS), as well as in inhibiting carbohydrate hydrolysing enzymes and the formation and accumulation of AGEs.[4-6] Consequently, their extraction from natural sources has attracted an exponential interest in recent years.[7,8]

Hazelnuts (*Corylus avellana* L.) belong to the *Betulaceae* family and, because of their appealing organoleptic and nutritional characteristics, are among the most consumed dry fruits in the world.[9] The global production exceeded 1.20 million tons in 2019.[10] Turkey is the leading producer, followed by Italy, USA and Azerbaijan.[10] Hazelnut shells (HZS), making up over half of the nut's weight, represent the major by-product. Their chemical analysis revealed a lignocellulosic composition (24.6–30% hemicelluloses, 27–27.3% cellulose, 40.7–43% lignin and 7.4% other components) that makes them suitable to be employed as boiler fuel or for biofuel production.[10] However, HZS valorization is fundamental to prevent significant economic losses and promote the onset of a robust circular economy around many sectors.[10] Significantly, earlier research has underscored the presence of key biomolecules in HZS, notably phenolic compounds, flavonoids and diarylheptanoids.[11] Nevertheless, maceration and ultrasound-assisted extraction (UAE), employing methanol or acetone as organic solvents[12-15] have been the only extraction methods investigated to recover bioactive compounds from HZS. So far, no research has examined the eco-friendly potential of microwave-assisted extraction (MAE) combined with the use of green solvents such as ethanol and water. Herein, MAE critical parameters were optimized by response surface methodology (RSM) to achieve the highest recovery of high-value antioxidants from *Corylus avellana* L. shells. Hence, the phytochemical profile of the resulting optimized extract (OHS-E), as well as its antiradical and anti-diabetic effects towards α-amylase, α-glucosidase and non-enzymatic glycation, were explored in detail, setting the stage for the development of new oral nutraceutical products through *in vitro* biocompatibility studies.

MATERIALS AND METHODS

Reagents

Milli-Q water (MilliporeSigma, Burlington, MA, USA) and chemicals of analytical (or superior) grade were employed in all the experiments, as received from commercial sources. Folin-Ciocalteau's phenol reagent, 1,1-diphenyl-2-picrylhydrazyl free radical ($DPPH^{\bullet}$) and 2,4,6-tri(2-pyridyl)-1,3,5-triazine (TPTZ) were acquired from Merck (Darmstadt, Germany). Trolox (6-hydroxy-2,-5,7,8-tetramethylchroman-2-carboxylic acid), potassium persulfate ($K_2S_2O_8$), 2,20-azino-bis(3-ethylbenzothiazoline-6-sulfonic acid) diammonium salt ($ABTS^{\bullet+}$), α-glucosidase from *Saccharomyces cerevisiae* (EC 3.2.1.20, Type I, lyophilized powder, ≥10 units mg^{-1} protein), porcine pancreatic α-amylase (EC 3.2.1.1, Type VI-B, >5 units mg^{-1} solid), *p*-nitrophenyl-α-D-glucopyranoside (*pNP-α-G*), starch from potato, 3,5-dinitrosalicylic acid (DNS), nitroblue tetrazolium chloride (NBT), β-nicotinamide adenine dinucleotide (NADH), sodium hypochlorite solution with 4% available chlorine, dihydrorhodamine 123 (DHR), phenazine methosulphate (PMS), α,α′-azodiisobutyramidine dihydrochloride (AAPH), fluorescein sodium salt, pyruvaldehyde solution and AG hydrochloride were purchased from Sigma-Aldrich (Steinheim, Germany), whereas catechin, gallic acid and Triton X-100 were purchased from Sigma Chemical Co. (St Louis, MO, USA). Dulbecco's modified Eagle's medium (DMEM), non-essential amino acids and Hank's balanced salt solution (HBSS) were purchased from Biowest SAS (Nuaillé, France). Fetal bovine serum (FBS) Supreme was obtained from PAN-Biotech (Aidenbach, Germany). TrypLE Express was obtained from Gibco (Life Technologies, SA, Madrid, Spain). Dimethylsulfoxide (DMSO) was purchased from AppliChem (Darmstadt, Germany).

Corylus avellana L. shells

HZS were kindly provided in December 2021 by a local supplier (Catania, Italy). HZS were mashed with an electrical grinder (Moongiantgo High-speed Multifunction Grinder, 2500 W, Lebanon, Tennessee, USA) and sifted through a 1 mm sieve to ensure uniformity. Hence, shell powder was stored at room temperature (293.15 K) in the dark until MAE. The yield of each extraction was calculated as:

$$Yield\ \% = \frac{weight\ dried\ shell\ extract\ (g)}{weight\ of\ starting\ shell\ powder\ (g)} \times 100 \qquad (1)$$

MAE

A microwave oven (S43 Type F322EC, RE; Smeg, Guastalla, Italy) equipped with a digital control screen to set up the desired irradiation time and MW power (150–1000 *W*) was employed. Aqueous ethanol in different concentrations was selected as GRAS solvent mixture. Briefly, 100 mg of HZS powder was mixed with the proper amount of solvent and subjected to MAE, following the Box–Behnken experimental design (BBD) reported in Table 1. The supernatant of each extract was filtered through cotton and dried in a vacuum concentrator (Concentrator plus/Vacufuge® plus; Eppendorf, Hamburg, Germany). All dried extracts were stored at 253.15 K until further measurements.

Experimental design for optimization

Single-factor experiments were initially carried out by varying one extraction parameter at a time when others were maintained constantly at a central value (70% EtOH, 120 *s*, 670 *W* and 30 mL g^{-1}). Subsequently, based on the total phenolic content (TPC) of the resulting extracts, preliminary factor levels (coded as −1, 0 and + 1) were selected and used to design experiments using response surface methodology (RSM). Hence, a four-factorial BBD was created using JMP® statistical software (SAS Institute Srl, Milano, Italy) to optimize the MAE parameters and obtain an extract with the highest TPC and antioxidant/antiradical activities (evaluated through $DPPH^{\bullet}$, ferric reducing antioxidant power (FRAP) and $ABTS^{\bullet+}$ assays). 27 experimental runs, including three replicates at the central point, were carried out according to Eqn (2):

$$N = 2k\,(k-1) + C_o \qquad (2)$$

where *N* is the number of experiments, *k* is the number of factors and C_0 is the number of central points.

J Sci Food Agric 2024; **104**: 9472–9485 © 2024 The Author(s). wileyonlinelibrary.com/jsfa
Journal of the Science of Food and Agriculture published by John Wiley & Sons Ltd on behalf of Society of Chemical Industry.

Table 1. Box–Behnken experimental design and results of the TPC and antioxidant/antiradical activities of MAE extracts from HZS

	Independent variables				Dependent variables			
	MAE conditions				Experimental data			
Run	X_1 (EtOH, % *v/v*)	X_2 (time, *s*)	X_3 (MW, *W*)	X_4 (ratio, mL g^{-1})	Y_1, TPC (mg GAE g^{-1} DW)	Y_2, FRAP (mg TE g^{-1} DW)	Y_3, DPPH (μg TE g^{-1} DW)	Y_4, ABTS (mg TE g^{-1} DW)
1	70	210	850	30	8.72 ± 0.50	1.09 ± 0.02	12.86 ± 0.21	1.54 ± 0.07
2	50	210	850	35	11.75 ± 0. 71	1.38 ± 0.05	15.88 ± 0.14	1.77 ± 0.08
3	50	120	850	40	8.24 ± 0.98	0.87 ± 0.01	12.16 ± 1.01	1.36 ± 0.02
4	70	210	670	35	10.49 ± 0.47	1.23 ± 0.04	14.48 ± 0.83	1.37 ± 0.03
5	20	120	850	35	7.41 ± 0.92	0.73 ± 0.02	11.75 ± 0.15	1.12 ± 0.27
6	20	210	670	35	13.02 ± 0.25	1.27 ± 0.03	16.32 ± 0.17	1.63 ± 0.06
7	50	120	670	35	9.87 ± 0.84	1.09 ± 0.02	12.61 ± 0.12	0.92 ± 0.14
8	50	210	1000	40	12.09 ± 0.45	1.18 ± 0.02	15.31 ± 0.13	1.72 ± 0.02
9	50	270	1000	35	12.55 ± 0.51	1.43 ± 0.05	16.71 ± 0.13	1.78 ± 0.05
10	50	210	1000	30	12.35 ± 0.32	1.31 ± 0.03	16.22 ± 0.46	1.95 ± 0.14
11	70	270	850	35	11.69 ± 0.50	1.43 ± 0.01	15.18 ± 0.88	1.71 ± 0.06
12	20	270	850	35	11.66 ± 0.54	1.35 ± 0.03	15.78 ± 0.21	1.80 ± 0.02
13	50	270	850	40	11.56 ± 0.85	1.55 ± 0.05	14.82 ± 1.37	2.27 ± 0.08
14	50	210	850	35	11.75 ± 0.43	1.37 ± 0.02	15.65 ± 0.07	1.79 ± 0.04
15	50	120	1000	35	10.22 ± 0.29	1.11 ± 0.01	13.56 ± 0.39	1.34 ± 0.05
16	50	210	670	40	12.35 ± 0.55	1.36 ± 0.04	16.25 ± 0.89	2.23 ± 0.04
17	50	210	850	35	11.74 ± 0.93	1.37 ± 0.04	15.77 ± 0.13	1.77 ± 0.03
18	70	210	850	40	10.28 ± 0.30	1.09 ± 0.02	12.73 ± 0.51	1.93 ± 0.01
19	50	270	670	35	13.40 ± 0.58	1.45 ± 0.02	16.86 ± 0.37	1.84 ± 0.10
20	20	210	850	40	10.46 ± 0.89	1.32 ± 0.06	16.32 ± 0.15	2.14 ± 0.12
21	20	210	1000	35	10.87 ± 0.85	1.31 ± 0.04	16.16 ± 1.33	1.93 ± 0.06
22	50	120	850	30	7.74 ± 0.37	0.76 ± 0.05	8.62 ± 0.08	1.13 ± 0.10
23	50	270	850	30	11.08 ± 0.82	1.18 ± 0.01	15.25 ± 0.86	1.95 ± 0.16
24	50	210	670	30	11.04 ± 0.23	0.98 ± 0.03	12.68 ± 0.21	1.28 ± 0.19
25	20	210	850	30	10.56 ± 0.76	0.78 ± 0.11	13.49 ± 0.25	1.99 ± 0.01
26	70	210	1000	35	12.70 ± 0.41	1.29 ± 0.02	15.27 ± 1.09	1.34 ± 0.04
27	70	120	850	35	8.22 ± 0.64	0.96 ± 0.03	10.84 ± 1.71	1.03 ± 0.09

HZS, *Corylus avellana* L. shells; TPC, total phenolic content; GAE, gallic acid equivalents; FRAP, ferric reducing antioxidant power; TE, Trolox equivalents.

To reduce the influence of systematic errors on the observed responses, a random order was followed to carry out the experiments. Consequently, data on the response variables (TPC, FRAP, $DPPH^{\bullet}$ and $ABTS^{\bullet+}$) were collected for each run of extraction and fitted to a second-order polynomial Eqn (3):

$$Y = B_0 + \sum_{i=1}^{k} B_i X_i + \sum_{i=1}^{k} B_{ii} X^2 + \sum_{i>j}^{k} B_{ij} X_i X_j + E \quad (3)$$

where Y is the response variable, X represents the independent variables (factors), B_0 is a constant coefficient, B_i, B_{ii} and B_{ij} are the linear, quadratic and interactive regression coefficients, respectively, and E represent the error term. The regression coefficients were calculated using the analysis of variance (ANOVA), with a p-value threshold of 0.05 (Tukey's test) being considered statistically significant. To assess the reliability of the developed model in navigating the experimental space, a signal-to-noise ratio (*S/N*), or adequate precision, greater than 4 was considered desirable.[16] Moreover, model efficiency was validated by considering the lack of fit, the coefficient of determination (R^2), the F-test values, as well as the coefficient of variation (CV). Lastly, the optimized extract from HZS (OHS-E) was obtained in triplicate under the estimated best factors combination.

Determination of TPC

TPC was spectrophotometrically determined using the Folin–Ciocalteu method, as previously reported.[7] Samples were dissolved in a MeOH/H_2O mixture (1:1, v/v) to a final concentration of 0.5 mg mL^{-1}. A standard calibration curve ($R^2 = 0.9994$) was achieved by testing gallic acid (0.05– 0.5 mg mL^{-1}) as sample. All mixtures were incubated at room temperature in darkness for 1 h and 30 min before the optical density (OD) was acquired at 765 nm. Results were achieved in quadruplicate and expressed as mg of gallic acid equivalents (GAE) per g of HZS dry weight (mg GAE g^{-1} DW).

In vitro antioxidant/antiradical activity

Ferric Reducing Antioxidant Power (FRAP) assay

HZS extracts' capacity to reduce a ferric-tripyridyltriazine (Fe^{3+}-TPTZ) complex to the blue-coloured ferrous form (Fe^{2+}-TPTZ) was spectrophotometrically evaluated following a previously detailed method.[8] Samples (0.5 mg mL^{-1}) and quercetin

 © 2024 The Author(s).
Journal of the Science of Food and Agriculture published by John Wiley & Sons Ltd on behalf of Society of Chemical Industry.

(0.1 mg mL^{-1}), were dissolved in a MeOH:H_2O mixture (1:1, *v/v*). Trolox (25–1000 μM) allowed the calibration curve to be obtained ($R^2 = 0.9979$). Blank solution was obtained by replacing samples with methanol. The OD was measured at 593 nm. The ferric reducing antioxidant power was determined in triplicate as:

$$\text{FRAP}\,(\%) = \frac{(OD_{blank} - OD_{sample})}{OD_{blank}} \times 100 \quad (4)$$

The results were expressed in mg of Trolox equivalents (TE) per gram of HZS dry weight (mg TE g^{-1} DW).

DPPH• scavenging capacity

The ability of HZS extracts in reducing the dark-violet coloured DPPH• radical into the yellow DPPH-H non-radical form was assessed following previously described procedures,[17,18] with minor modifications. Extracts from HZS (0.5 mg mL^{-1}) and quercetin (0.05 mg mL^{-1}) were dissolved in a MeOH:H_2O mixture (1:1, v/v). Trolox (0.1–0.8 mM) was employed for the calibration curve ($R^2 = 0.9986$). The OD was measured at 515 nm. The DPPH radical scavenging percentage was given by Eqn (5):

$$\text{DPPH}^{\bullet}\ \text{scavenging}\,(\%) = \frac{(OD_{blank} - OD_{sample})}{OD_{blank}} \times 100 \quad (5)$$

where OD_{blank} and OD_{sample} are the optical densities measured in absence or presence of extracts/control, respectively. Therefore, results were obtained in triplicate and expressed as μg of TE per gram of HZS dry weight (μg TE g^{-1} DW).

$ABTS^{\bullet+}$ scavenging capacity

The $ABTS^{\bullet+}$ scavenging capacity of HZS extracts was evaluated following previously described methods,[17,18] with slight modifications. Briefly, samples (0.1 mg mL^{-1}) or quercetin (0.4 mg mL^{-1}) were dissolved in a EtOH/H_2O mixture (1:1, *v/v*). A calibration curve of Trolox (25–200 μM) was achieved ($R^2 = 0.9981$). The OD was measured at 734 nm after an incubation time of 6 min in the dark. The $ABTS^{\bullet+}$ scavenging capacity of each sample was calculated by Eqn (6). Hence, results were obtained in triplicate and expressed as mg of TE per gram of HZS dry weight (mg TE g^{-1} DW).

$$\text{ABTS}^{\bullet+}\ \text{scavenging}\,(\%) = \frac{(OD_{blank} - OD_{sample})}{OD_{blank}} \times 100 \quad (6)$$

Liquid chromatography (LC)-mass apectrometry (MS) analysis of OHS-E

HPLC/electrospray ionozation (ESI)-MS/MS analysis of OHS-E was carried out on a linear ion trap mass spectrometer (LTQ; Thermo Fisher Scientific, San Jose, CA, USA), following the methodologies proposed in our previous studies.[7,8] OHS-E was dissolved in aqueous methanol (1:1, *v/v*) at 40 mg mL^{-1}. The instrument was equipped with an ESI source operating in negative mode. The elution was conducted using a Symmetry RP-C18 column (Waters Corp., Milford, MA, USA) (150 mm × 1 mm inner diameter, 100 Å, 3.5 μm) maintained at 298.15 K. The solvents used were H_2O + 1% formic acid (solvent A) and acetonitrile + 1% formic acid (solvent B). The solvent gradient of B was 0 min, 5% B; 25 min, 15% B; 40 min, 25% B; 55 min, 55% B; 60 min, 95% B, 65 min 100% B; 80 min, 5% B. Flow rate and injection volume were at 0.50 mL min^{-1} and 20 μL, respectively. The ionization parameters were established as: capillary temperature, 493.15 K; sheath gas, 30 arbitrary units; source voltage, 4 kV; and capillary voltage, −20 V.

The putative identification of compounds was obtained considering the MS/MS elution times (r_t), $[M - H]^-$ *m/z* values, MS/MS fragmentation patterns and relative abundances, as well as by comparing our MS data with those reported in the literature. Tentative identification of fatty acids was achieved by comparing the molecular masses with the information retrieved from LIPID MAPS® Structure Database (LMSD) (https://www.lipidmaps.org; accessed February 2024). Moreover, diagnostic fragmentation patterns were considered. The quantitative analysis of selected components was performed using the following standards calibration curves (concentration range = 0.1–6.3 × 10^{-4} μg mL^{-1}):

$$\text{Gallic acid}\ y = 1\times10^{7}x + 96640; R^2 = 0.9932$$

$$\text{Quercetin-3-}O\text{-glucoside}\ y = 2\times10^{8}x + 1\times10^{7}; R^2 = 0.9996$$

$$(\text{C18:2})\text{-Linoleic acid}\ y = 1\times10^{8}x + 2\times10^{6}; R^2 = 1$$

The results were calculated considering the peak area of the molecular ions and were expressed as mg of organic compound per gram of HZS dry weight (mg g^{-1} DW).

ROS scavenging assays

Superoxide radical anion ($O_2^{\bullet-}$) scavenging assay

$O_2^{\bullet-}$ scavenging ability of OHS-E was measured using a previously detailed spectrophotometric method.[19] OHS-E (15.63–500 μg mL^{-1}), catechin (7.81–250 μg mL^{-1}) and gallic acid (0.98–15.63 μg mL^{-1}) were dissolved in phosphate buffer (19 mM, pH 7.4). A blank solution was obtained by replacing the sample/control with the same volume of phosphate buffer. The OD was measured at 560 nm over 2 min. The $O_2^{\bullet-}$ scavenging capacity of OHS-E was achieved according to Eqn (7). Therefore, the concentration required to inhibit 50% of the $O_2^{\bullet-}$-induced NBT reduction (IC_{50} μg mL^{-1}) was calculated in triplicate by regression analysis.

$$O_2^{\bullet-}\ \text{scavenging}\,(\%) = \frac{(OD_{blank} - OD_{sample})}{OD_{blank}} \times 100 \quad (7)$$

Hypochlorous acid (HClO) scavenging assay

The efficacy of OHS-E in preventing the conversion of DHR to rhodamine induced by HClO was spectrophotometrically assessed using a previous method.[19] Different solutions of OHS (15.63–500 μg mL^{-1}), gallic acid (0.98–15.63 μg mL^{-1}) and catechin (0.25–3.91 μg mL^{-1}) were obtained in phosphate buffer (100 mM, pH 7.4). A blank solution was obtained by replacing sample/controls with phosphate buffer. The OD was acquired at λ_{ex} = 485 nm and λ_{em} = 528 nm. Results were obtained in triplicate according to Eqn (8) and expressed in terms of IC_{50} (μg mL^{-1}) by regression analysis.

$$\text{HClO scavenging}\,(\%) = \frac{(OD_{blank} - OD_{sample})}{OD_{blank}} \times 100 \quad (8)$$

Oxygen radical absorbance capacity (ORAC) assay

The ORAC assay was performed on OHS-E, following previously detailed methods.[8,19] OHS-E was serial diluted from 15.62 to 0.98 μg mL^{-1} in phosphate buffer (75 mM, pH 7.5). Catechin

 © 2024 The Author(s).
Journal of the Science of Food and Agriculture published by John Wiley & Sons Ltd on behalf of Society of Chemical Industry.

(0.02–0.2 μg mL^{-1}) and gallic acid (0.18–1.5 μg mL^{-1}) served as positive controls. Trolox (0.19–1.5 μg mL^{-1}) was employed to achieve a calibration curve ($R^2 = 0.9923$). The fluorescence decrease was monitored at 310.15 K every minute for 120 min ($\lambda_{ex} = 485$ nm; $\lambda_{em} = 528$). The area under the fluorescence decay curves (AUC) of extract/positive controls was calculated using Eqn (9):

$$AUC = 1 + {}^{f_1}\!/_{f_0} + {}^{f_2}\!/_{f_0} + {}^{f_3}\!/_{f_0} \ldots + {}^{f_i}\!/_{f_0} \quad (9)$$

where f_0 is the initial fluorescence measured at 0 min and f_i is the fluorescence measured at time *i*. Therefore, the net AUC was obtained by subtracting the AUC of the blank from that of the sample/control. Results were calculated in triplicate and expressed as μmol of TE per mg of HZS dry weight (μmol TE mg^{-1} DW).

In vitro biological activities

α-Amylase inhibition

The inhibition efficiency of OHS-E towards α-amylase was investigated following the methodology proposed in our previous study.[8] Detailed assay conditions are reported in the Supporting information (section 1.1). The α-amylase inhibition percentage of OHS-Ewas calculated in triplicate according to Eqn (10):

$$\text{Inhibition}\,(\%) = \frac{(OD_{blank} - OD_{sample})}{OD_{blank}} \times 100 \quad (10)$$

Hence, IC_{50} was obtained by regression analysis and expressed in μg mL^{-1}.

α-Glucosidase inhibition

The α–glucosidase inhibition capacity of OHS-E was evaluated using a previously described method, with slight modifications.[20] Detailed assay conditions are reported in the Supporting information (section 1.2). Results were obtained in triplicate according to Eqn (10). Regression analysis using linear fitting allowed to achieve the IC_{50} value (μg mL^{-1}).

Inhibition of AGE formation

The inhibitory efficacy of OHS-E towards AGE formation was tested by three different reaction systems, following the method of Wang *et al.*,[2] with slight modifications. OHS-E, AG or catechin (positive controls) were dissolved in phosphate buffer (50 mM, pH 7.4, with 0.02% sodium azide) and serially diluted from 1.5 to 0.15 mg mL^{-1} for IC_{50} determination. The results were obtained in triplicate and presented even as AGE inhibition percentage (%), calculated using Eqn (11):

$$\text{Inhibition of fluorescent AGEs}\,(\%) = \frac{F_0 - F}{F_0} \times 100 \quad (11)$$

where F and F_0 represent the fluorescence intensity with and without OHS-E/controls, respectively. Human serum albumin (HSA)/fructose and HSA/methylglyoxal reaction systems allowed the evaluation of all the stages of protein glycation, whereas arginine was employed as the major source of AGEs in the arginine/methylglyoxal reaction model. Assay conditions applied in each reaction system are detailed in the Supporting information (section 1.3).

In vitro intestinal cell viability

Cell cultures

Caco-2 (ATCC Number: HTB-37; age, 72 years; Caucasian; male;) and HT29-MTX (ATCC Number: HTB-38; age, 44 years; Caucasian; female) colon epithelial cells were obtained from the American Type Culture Collection (ATCC, Manassas, VA, USA). Both cell lines were individually grown in tissue culture flasks (Orange Scientific, Belgium) at 310.15 K in a 5% CO_2 environment (CellCulture® CO_2 Incubator; ESCO GB Ltd, Barnsley, UK) until 90–95% confluence. Cells were maintained in DMEM supplemented with 10% (*v/v*) FBS, 1% (*v/v*) antibiotic–antimitotic mixture (100 U mL^{-1} penicillin +100 U mL^{-1} streptomycin), 1% (*v/v*) L-glutamine and 1% (*v/v*) non-essential amino acids. Every 48 h, cells were washed with HBSS and fresh medium was supplied.

3-(4,5-Dimethylthiazol-2-yl)-2,5-diphenyltetrazolium bromide (MTT) assays

Biocompatibility of OHS-E towards human intestinal cells was evaluated by MTT assays, following previously reported procedures.[6,8] Caco-2 (passages 23–24) and HT29-MTX (passages 84–85) were prepared in DMEM at 1×10^5 cells mL^{-1} and incubated into a 96-well microplate for 48 h. OHS-E (62.5 to 1000 μg mL^{-1}) was dissolved in DMEM and put in contact with cells for 24 h. DMEM and 1% (*w/v*) Triton X-100 were used as the positive and negative control, respectively. After 24 h of incubation, cells were washed with HBSS. MTT reagent (0.5%, *w/v*) was added, and the plate was incubated for 3 h at 310.15 K, protected from light. DMSO was used to dissolve the insoluble purple formazan product. Hence, the percentage of cell viability was quantitatively determined in quadruplicate by reading the OD at 570 nm, with a background subtraction at 690 nm. The results were achieved in quadruplicate and expressed as percentages of cell viability (%).

Statistical analysis

All experiments were conducted at least in triplicate, and results were expressed as the mean ± SD. OriginPro 2023 software (OriginLab Corp., Northampton, MA, USA) was adopted for the one-way ANOVA. According to Tukey's test, sample differences were considered statistically significant when $p < 0.05$.

RESULTS AND DISCUSSION

Optimization of MAE conditions

Single-factor experiments

In the present study, single-factor experiments were conducted to select the preliminary range of the most relevant independent variables affecting the MAE of compounds from HZS, defining the experimental space. The appropriate choice of the experimental space represents the first critical step to ensure the development of an efficient predictive regression model. The factor ranges examined during these pilot experiments are summarized in the Supporting information (Table S1).

As shown in Table 2, the ethanol concentration significantly affected the TPC of HZS extracts during MAE, with 20% aqueous ethanol providing a higher recovery (10.32 mg GAE g^{-1} DW) than 80% (6.88 mg GAE g^{-1} DW) and 90% (3.11 mg GAE g^{-1} DW). This behaviour could be attributed to a major solubility of phenolic compounds in a polar medium like water, whereas high alcoholic concentrations could prevent their dissolution from the shell matrix due to protein denaturation.[20] Consequently, the optimization design has explored the ethanol concentration between 20% and 70%.

© 2024 The Author(s).

Journal of the Science of Food and Agriculture published by John Wiley & Sons Ltd on behalf of Society of Chemical Industry.

Table 2. Results of the single-factor experiments for MAE from *Corylus avellana* L. hard shells and results of ANOVA with Tukey's test

EtOH concentration (X_1)		Irradiation time (X_2)		MW power (X_3)		Solvent-to-powder ratio (X_4)	
(% *v/v*)	TPC	(*s*)	TPC	(*W*)	TPC	(mL g^{-1})	TPC
20	10.32 ± 0.53^{a}	50	5.96 ± 0.33^{a}	150	4.20 ± 0.88^{b}	20	5.08 ± 0.69^{b}
50	9.84 ± 0.21^{a}	90	6.04 ± 0.41^{c}	430	4.52 ± 0.11^{c}	25	5.56 ± 0.26^{c}
70	7.00 ± 0.27^{b}	120	7.08 ± 0.15^{ab}	670	6.84 ± 0.45^{bc}	30	6.94 ± 0.21^{c}
80	6.88 ± 0.17^{b}	210	10.48 ± 0.17^{a}	850	10.65 ± 0.31^{a}	35	9.43 ± 0.14^{b}
90	3.11 ± 0.63^{c}	270	8.07 ± 0.47^{b}	1000	7.52 ± 0.12^{b}	40	10.24 ± 0.10^{a}

Values are reported as the mean ± SD ($n = 4$). Data are expressed as equivalent of gallic acid (GAE) in mg g^{-1} of dried extract (mg GAE g^{-1} DW). Mean values in a column with different lowercase letters are statistically different for $p < 0.05$ (Tukey's test).

By increasing the irradiation time from 50 *s* to 270 *s*, the TPC increased from 5.96 to 10.48 mg GAE g^{-1} DW (Table 2). This behaviour could be attributed to inadequate dielectric heating at 50 and 90 *s*.[22] Consequently, 120, 210 and 270 *s* were the lower, middle, and upper levels selected to develop the BBD model.

Concerning MW power, results showed that TPC increased as MW power increase, reaching a maximum of 10.64 mg GAE g^{-1} DW at 850 *W*, followed by a decrease at 1000 *W* (8.07 mg GAE g^{-1} DW), probably because of the solvent overheating.[21] Based on these results, 670–1000 *W* was the preliminary range adopted in the BBD for the optimization phase.

The solvent/powder ratio represents the last crucial variable for an optimal MAE of phytochemicals from HZS. Notably, TPC increased from 5.08 to 10.24 mg GAE g^{-1} DW by increasing the solvent/powder ratio from 20 to 40 mL g^{-1}. Nayak *et al.*[23] previously described a similar trend, attributing this behaviour to the poor MW absorption and heating occurring with low solvent volumes. Hence, 30–40 mL g^{-1} was the preliminary range explored in the following MAE experiments. An overview of all preliminary factor ranges selected during single-factor experiments can be found in the Supporting information (Table S2).

Effects of the extraction variables on TPC and antioxidant activity of HZS extracts

In this study, RSM was employed to establish the most effective MAE conditions to maximize TPC and antioxidant/antiradical activity of HZS. The main factors, namely ethanol concentration (X_1), irradiation time (X_2), MW power (X_3) and solvent-to-powder ratio (X_4), as well as their preliminary ranges, were defined according to single-factor experiments (Table 2). The applied MAE conditions and the corresponding data on the measured responses (Y_1 – Y_4) are shown in Table 1. As can be noticed, TPC changed from 7.41 (run 5) to 13.40 mg GAE g^{-1} DW (run 19); FRAP ranged between 0.73 (run 5) to 1.55 mg TE g^{-1} DW (run 13); DPPH$^{\bullet}$ varied from 8.62 (run 22) to 16.86 µg TE g^{-1} DW (run 19); whereas ABTS$^{\bullet+}$ changed from 0.92 (run 7) to 2.27 mg TE g^{-1} DW (run 13).

The model adequacy, as well as the significance ($p < 0.05$) of both primary and interactive effects of each factor under study were evaluated through ANOVA. As indicated in Table 3, the coefficients of determination (R^2) were higher than 0.9438 for all the responses. Nevertheless, a high R^2 alone does not ensure the reliability of the regression model. For a robust BBD, the adjusted R^2 (R^2 adjusted) should be close to R^2. Our R^2 and R^2 adjusted values closely matched each other. Furthermore, the not significance ($p > 0.05$) of the lack of fit (Table 3) and a coefficient of variation (CV %) of 2.87% supported the model's validity as well. Adequate precision values, reflecting the signal-to-noise (*S/N*) ratio, were higher than 4, corroborating the model's reliability and reproducibility.[7,16]

According to Table 3, all the linear coefficients significantly impacted the response variables. However, irradiation time (X_2) exhibited the highest *F*-values of 205.05 (Y_1), 142.77 (Y_2), 256.28 (Y_3) and 164.22 (Y_4), being the independent variable that mostly affected TPC and antioxidant/antiradical activities of HZS. Among the interactive regression coefficients, X_1X_2, X_2X_3 and X_2X_4 terms significantly ($p < 0.05$) affected all dependent variables. Regarding quadratic terms, X_2X_2 and X_4X_4 were significant ($p < 0.05$) for all responses. Excluding the not significant coefficients ($p > 0.05$), the final predictive equations [Eqn (12) to (15)] were obtained as follows:

$$Y_1(\text{TPC}) = -17.782 - 0.194x_1 + 0.084x_2 - 0.056x_3 + 2.641x_4 - 1.58\times10^{-4}x_2^2 - 0.033x_4^2 - 1.6\times10^{-4}x_1x_2 - 1.8\times10^{-4}x_2x_3 + 0.003x_2x_4 \quad (12)$$

$$Y_2(\text{FRAP}) = -16.306 + 0.059x_1 + 0.710x_2 + 0.052x_3 + 0.069x_4 - 1.5\times10^{-5}x_2^2 - 0.007x_4^2 - 2.6\times10^{-4}x_1x_2 - 1.7\times10^{-4}x_2x_3 - 0.001x_2x_4 \quad (13)$$

$$Y_3(\text{DPPH}) = -119.221 + 0.258x_1 + 0.208x_2 + 0.004x_3 + 5.761x_4 - 2.2\times10^{-4}x_2^2 - 0.052x_4^2 + 5.7\times10^{-4}x_1x_2 + 6.2\times10^{-4}x_2x_3 - 0.003x_2x_4 \quad (14)$$

$$Y_4(\text{ABTS}) = -8.707 + 0.012x_1 + 0.024x_2 + 0.022x_3 - 0.148x_4 - 1.9\times10^{-4}x_1^2 - 3.2\times10^{-5}x_2^2 + 0.006x_4^2 - 0.007x_1x_2 - 0.003x_2x_3 + 6.24\times10^{-4}x_2x_4 \quad (15)$$

3D Response surface analysis

In this study, 3D response surface plots derived from the above-mentioned predictive equations were used to investigate the interactive effects of two paired MAE parameters on TPC (Fig. 1a), FRAP (Fig. 1b), DPPH$^{\bullet}$ (Fig. 1c) and ABTS$^{\bullet+}$ (Fig. 1d) values exhibited by HZS extracts. These graphs enable fixing two variables at their central level, whereas the other two can be simultaneously adjusted, providing a comprehensive view of each factor's impact. Specifically, Fig. 1 shows that both TPC and antioxidant/antiradical activities of HZS improved when MW power ranged between 670 and 700 *W*, for irradiation times exceeding

 © 2024 The Author(s).
Journal of the Science of Food and Agriculture published by John Wiley & Sons Ltd on behalf of Society of Chemical Industry.

Table 3. ANOVA results from the BBD model for TPC (Y_1) and antioxidant/antiradical activities evaluated by FRAP (Y_2), DPPH (Y_3) and ABTS (Y_4) assays for HZS

	Sum of squares				*F*-values				*p*-values			
Variable	Y_1	Y_2	Y_3	Y_4	Y_1	Y_2	Y_3	Y_4	Y_1	Y_2	Y_3	Y_4
Model	67.66	1.24	107.74	3.40	29.01	28.77	39.57	24.45	<0.0001*	<0.0001*	<0.0001*	<0.0001*
X_1	4.44	0.09	5.88	0.2	26.68	16.32	30.22	20.41	0.0002*	0.0016*	<0.0001*	0.0007*
X_2	34.16	0.68	49.84	1.63	205.05	142.77	256.28	164.22	<0.0001*	<0.0001*	<0.0001*	<0.0001*
X_3	5.02	0.06	1.18	0.09	30.17	12.09	6.07	9.22	0.0001*	0.0046*	0.0298*	0.0103*
X_4	3.74	0.17	10.84	0.27	22.49	34.90	55.72	26.71	0.0005*	<0.0001*	<0.0001*	0.0002*
X_1X_2	4.62	0.06	5.01	0.35	27.71	12.04	25.74	35.32	0.0002*	0.0029*	0.0003*	<0.0001*
X_1X_3	0.06	2×10^{-4}	0.27	0.02	0.29	0.05	1.38	2.38	0.0631	0.8152	0.2637	0.1487
X_2X_3	0.91	0.02	1.59	0.11	4.24	17.01	10.97	14.42	0.0477*	0.0022*	0.0046*	0.0026*
X_1X_4	1×10^{-4}	6×10^{-5}	0.18	2×10^{-3}	1×10^{-3}	2.64	0.98	0.23	0.9739	0.1300	0.3623	0.6428
X_2X_4	3.62	0.08	2.21	0.06	20.69	16.52	11.38	5.82	0.0005*	0.0016*	0.0055*	0.0328*
X_3X_4	0.36	0.01	4×10^{-4}	8×10^{-4}	2.16	2.11	2.5×10^{-3}	0.08	0.1671	0.1724	0.9611	0.7786
X_1X_1	0.38	0.01	0.13	0.07	2.29	2.56	21.23	6.87	0.1562	0.1357	0.3971	0.0223*
X_2X_2	3.79	0.03	7.63	0.16	22.79	6.03	39.22	15.7	0.0004*	0.0303*	<0.0001*	0.0019*
X_3X_3	0.04	1×10^{-3}	2.53	0.04	0.24	0.35	13.03	3.91	0.0634	0.5648	0.0036*	0.0617
X_4X_4	0.84	0.17	9.06	0.14	4.55	35.30	46.59	13.59	0.0465*	<0.0001*	<0.0001*	0.0031*
Lack of fit	0.89	0.08	2.50	0.22	3.52	4.84	1.54	19.27	0.0883	0.6193	0.0613	0.0842
R^2	0.97	0.94	0.98	0.97								
R^2 (adjusted)	0.94	0.91	0.95	0.93								
S/N ratio	24.71	15.1	23.9	16.5								

X_1, solvent concentration (%, *v/v*); X_2, irradiation time (*s*); X_3, MW power (*W*); X_4, solvent-to-powder ratio (mL g^{-1}).
*Values are statistically significant at $p < 0.05$ (Tukey's test).

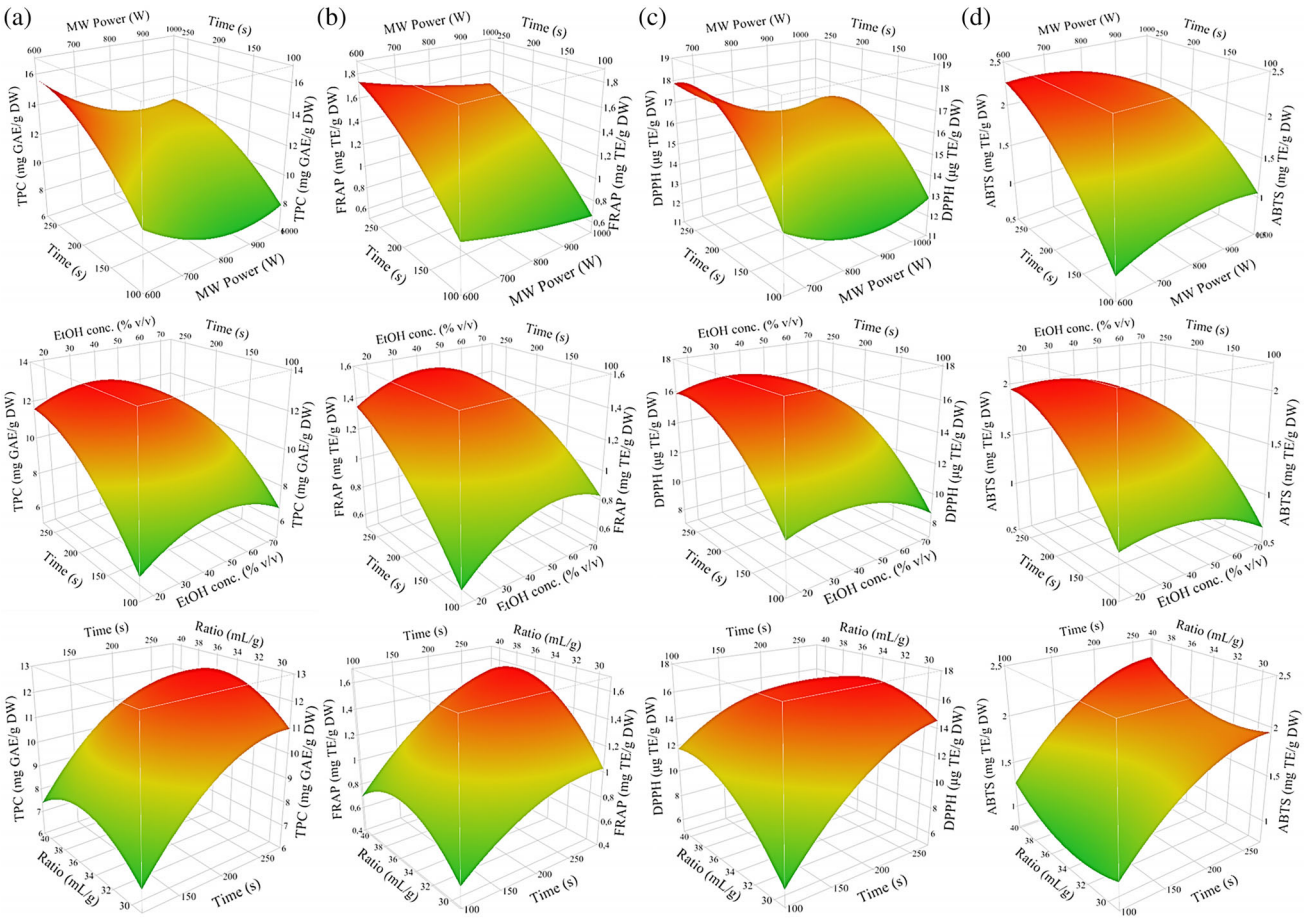


Figure 1. 3D response surface graphs for the significant ($p < 0.05$) interaction effects of ethanol concentration (% *v/v*), irradiation time (*s*), MW power and solvent/powder ratio (mL g^{-1}) on TPC (a), FRAP (b), $DPPH^{\bullet}$ (c) and $ABTS^{\bullet+}$ (d).

 © 2024 The Author(s).
Journal of the Science of Food and Agriculture published by John Wiley & Sons Ltd on behalf of Society of Chemical Industry.

250 *s*. Conversely, MW power around 1000 *W* led to a decrease in all responses, supporting the observations from our prior single-factor experiments (Table 2). Lower MW energy could promote a more gradual and uniform heating, reducing the risk of degradation of thermolabile compounds. These results aligned with Dahmoune *et al*., who also observed a TPC decline at MW powers higher than 600 *W*.[21]

According to Table 3, the interaction between ethanol concentration and irradiation time (X_1X_2 term) significantly ($p < 0.05$) affected all response variables. Notably, Fig. 1 shows that all responses were maximized by increasing time from 120 to 270 *s*, with an ethanol concentration ranging between 20 and 30%. This solvent concentration resulted in ideal, presumably a result of the water-induced swelling of the solid phase, combined with the amphiphilic properties of ethanol, which promote the migration of both polar and non-polar compounds.[24] Lastly, Fig. 1 illustrates all responses raised by increasing the solvent/powder ratio from 30 to 40 mL g^{-1} and prolonging the extraction time above 250 *s*. This improvement could be attributed to a steeper concentration gradient promoted by larger solvent volumes.[25] The 3D response surface plots for TPC, FRAP, DPPH$^{\bullet}$ and ABTS$^{\bullet+}$ as a function of the not significant interaction terms are provided in the Supporting Information (Fig. S1).

Validation of the predictive BBD model

Based on the above-mentioned predictive equations and ANOVA results, the best point of balance leading to the maximum TPC was estimated to be 26.7% (*v/v*) of ethanol in water concentration, 270 *s*, 670 *W* and 36.1 mL g^{-1}. The expected optimal MAE conditions for FRAP were 29.9% EtOH, 270 *s*, 670 *W* and 36.6 mL g^{-1}; those for DPPH$^{\bullet}$ were 23.8% EtOH, 258.5 *s*, 670 *W* and 36.5 mL g^{-1}; and those for ABTS were 32.7% EtOH, 270 *s*, 670 *W* and 40 mL g^{-1}. Accordingly, 28% (*v/v*) of ethanol in water concentration, 270 *s*, 670 *W* and 37 mL g^{-1} were the optimal parameters for the MAE of bioactive compounds from HZS. Under these conditions, the model estimated a maximum TPC of 14.28 mg GAE g^{-1} DW, a FRAP value of 1.67 mg TE g^{-1} DW, a DPPH$^{\bullet}$ value of 17.86 µg TE g^{-1} DW and an ABTS$^{\bullet+}$ result of 2.50 mg TE g^{-1} DW, respectively. MAE was carried out under the predicted optimal conditions to validate such results. The resulting OHS-E exhibited an experimental TPC of 15.12 mg GAE g^{-1} DW, higher than the one reported by Yuan *et al*.[12] (11.23 mg GAE g^{-1} DW) for a hazelnut shell extract prepared by UAE using an extraction time of 4 h, 61% of acetone concentration and a solid/liquid ratio of 10 g L^{-1}. Concerning antioxidant/antiradical activities, OHS-E exhibited FRAP, DPPH$^{\bullet}$ and ABTS$^{\bullet+}$ values of 1.58 mg TE g^{-1} DW, 18.43 µg TE g^{-1} DW and 2.64 mg TE g^{-1} DW, respectively. Lower FRAP values, ranging from 0.21 to 0.68 mg TE g^{-1}, were reported by Di Michele *et al*.[14] for hazelnut shell extracts obtained by maceration, UAE and high-power UAE in ethanol. Overall, the experimental values closely matched the predicted ones ($p < 0.05$) (see Supporting information, Table S3), suggesting the validity of the regression model to be applied for the MAE of bioactive compounds from HZS.

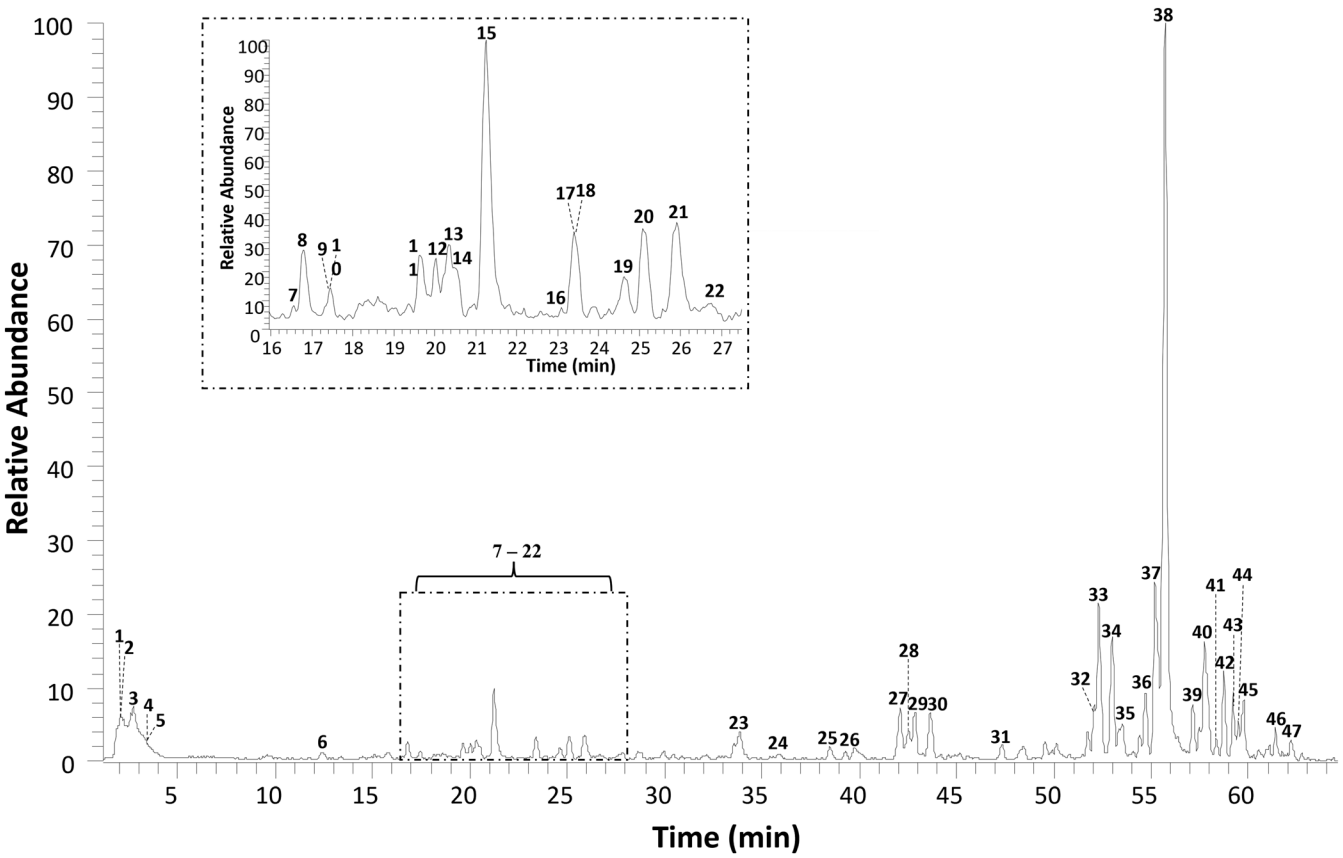


Figure 2. HPLC/ESI-MS/MS profile (negative ion mode) of the optimized extract from *C. avellana* shells (OHS-E). Peak identifications are reported in Table 4.

© 2024 The Author(s).
Journal of the Science of Food and Agriculture published by John Wiley & Sons Ltd on behalf of Society of Chemical Industry.

Table 4. Tentative identification by HPLC/ESI-MS/MS of the main organic constituents of the optimized extract from *C. avellana* shells (OHS-E)

Peak	t_r	$[M-H]^-$ (*m/z*)	Fragments, *m/z* (Relative intensity)	Proposed identification	mg g^{-1} of extract DW
1	2.40	133	115(100); 89 (5)	Malic acid	
2	2.40	209	191 (100); 85 (20); 173 (5); 129 (5)	D-Glucaric acid	
3	2.70	191	111 (100); 173 (40)	Quinic acid	
4	3.50	169	125 (100)	Gallic acid	
5	3.50	179	161 (100); 164 (10)	Coniferyl alcohol	
6	13.4	361	241 (100); 271 (30); 301 (20); 343 (10)	Giffonin P	
7	16.1	359	341 (100); 329 (60)	Giffonin U	
8	16.7	173	111 (100); 155 (5)	Shikimic acid	4.84 ± 0.24[a]
9	17.5	301	257 (100); 229 (50); 284 (30); 185 (20)	Ellagic acid	
10	17.5	225	210 (100)	Pinosylvin monomethyl ether	
11	19.6	221	162 (100); 206 (40); 150 (5)	Isofraxidin	
12	20.0	419 [M + HCOOH]-H]$^-$	195 (100); 373 (60); 325 (20); 177 (20)	Erythro-guaiacylglycerol-*β*-coniferyl aldehyde ether	
13	20.4	343	270 (100); 285 (40); 298 (20); 257 (20); 313 (10)	Dihydroxy-trimethoxy flavone	
14	20.4	447	301 (100); 300 (20); 302 (5)	Quercetin-O-rhamnoside	
15	21.2	187	125 (100); 169 (10); 143 (5)	Gallic acid derivative	27.30 ± 0.09[a]
16	23.1	375	345 (100); 357 (10)	7-Hydroxylariciresinol	
17	23.4	431	285 (100); 255 (10)	Kaempferol-3-O-rhamnoside	
18	23.4	476	433 (100); 462 (80); 315 (60); 337 (20); 279 (20); 235 (10)	1-Linoleoyl-sn-glycero-3-phosphoethanolamine	
19	24.5	555	525 (100); 507 (40); 329 (15); 315 (5); 195 (5)	Lariciresinol guaiacylglyceryl ether	
20	25.1	343	325 (100); 299 (20); 269 (20); 283 (5)	Carpinontriol B	
21	25.9	601	583 (100); 301 (20); 273 (5); 271 (5)	Gallagic acid dilactone	10.76 ± 0.02[a]
22	26.9	327	253 (100); 283 (80); 271 (30); 312 (20); 241 (20)	Giffonin V	
23	33.9	583	369 (100); 357 (49); 373 (20); 195 (20)	G(*β*–O–4′)S(*β*–5′)G-lignin oligomer	
24	35.8	215	197 (100); 153 (40); 171 (10); 169 (5)	(C12:0) Hydroxy-dodecanoic acid isomer	
25	38.5	327	309 (100); 291 (80); 183 (20); 239 (15); 115 (5)	(C18:2) Trihydroxy-octadecadienoic acid isomer	0.53 ± 0.01[c]
26	39.7	327	291 (100); 309 (60); 211 (60); 239 (20); 183 (10); 115 (5)	(C18:2) Trihydroxy-octadecadienoic acid isomer	
27	42.1	329	229 (100); 211 (60); 311 (40); 285 (20); 171 (20); 183 (10)	(C18:1) Trihydroxy-octadecenoic acid isomer	
28	42.6	329	229 (100); 211 (60); 311 (40); 285 (20); 171 (20); 183 (10)	(C18:1) Trihydroxy-octadecenoic acid isomer	
29	43.0	287	269 (100); 243 (10)	(C16:0) Dihydroxy-hexadecanoic acid isomer	
30	43.6	577	285 (100); 431 (10)	Kaempferol-3-O-(4″-p-coumaroyl)-*α*-rhamnopyranoside	0.87 ± 0.01[b]
31	47.3	313	295 (100); 245 (10); 171 (10); 213 (5)	(C17:2) Trihydroxy-heptadecadienoic acid isomer	1.75 ± 0.01[c]
32	52.0	377	359 (100); 333 (10); 362 (5)	(C25:2) Methyl-tetracosadienoic acid isomer	6.54 ± 0.02[c,d]
33	52.4	313	295 (100); 245 (20); 213 (10); 171 (10)	(C17:2) Trihydroxy-heptadecadienoic acid isomer	6.54 ± 0.02[c,d]
34	53.0	359	315 (100); 341 (40); 323 (20)	(C22:6) Dihydroxy-docosahexaenoic acid isomer	3.36 ± 0.011[c]
35	53.5	387	315 (100); 343 (20); 369 (10)	(26:4) Hexacosatetraenoic acid isomer	
36	54.7	315	297 (100); 295 (20); 279 (20); 271 (10)	(C18:0) Dihydroxystearic acid isomer	1.87 ± 0.037[c]
37	55.2	265	97 (100); 221 (10); 247 (5)	(C17:2) Heptadecynoic acid isomer	
38	55.7	315	297 (100); 295 (60); 279 (20); 271 (10)	(C18:0) Dihydroxystearic acid isomer	26.31 ± 0.081[c]
39	57.2	279	97 (100); 261 (10); 235 (10)	(C18:2) Linoleic acid	1.29 ± 0.007[c]
40	57.8	309	97 (100); 265 (20); 291 (10)	(C20:1) Eicosenoic acid isomer	3.96 ± 0.052[c]

© 2024 The Author(s).

Journal of the Science of Food and Agriculture published by John Wiley & Sons Ltd on behalf of Society of Chemical Industry.

Table 4. Continued

Peak	t_r	$[M-H]^-$ (*m/z*)	Fragments, *m/z* (Relative intensity)	Proposed identification	mg g^{-1} of extract DW
41	58.3	311	183 (100); 293 (10); 253 (10); 267 (5); 223 (5); 171 (5)	(C18:2) Dihydroxy-octadecadienoic acid isomer	0.41 ± 0.002[c]
42	58.7	353	291 (100); 309 (40); 335 (40)	(C23:0) Tricosanoic acid isomer	2.09 ± 0.023[c]
43	59.2	397	379 (100); 353 (80)	(C25:0) Hydroxy-pentacosanoic acid	
44	59.5	325	183 (100); 307 (20); 281 (20);225 (5)	(C21:0) Heneicosanoic acid isomer	
45	59.8	293	251 (100); 221 (40); 249 (20); 207 (5)	(C18:3) Hydroxy-octadecatrienoic acid isomer	
46	61.4	337	293 (100); 319 (40); 97 (20)	(C22:1) Erucic acid	0.68 ± 0.005[c]
47	62.2	381	337 (100); 363 (80)	(C25:0) Pentacosanoic acid	0.37 ± 0.003[c]

[a] Quantified as gallic acid.
[b] Quantified as quercetin-3-*O*-glucoside.
[c] Quantified as (C18:2)-linoleic acid.
[d] Quantified together.

Table 5. Inhibitory activity towards α-amylase (α-Amy) and α-glucosidase (α-Glu) and reactive oxygen species (ROS) scavenging capacity of OHS-E

Hypoglycaemic activity			Reactive oxygen scavenging capacity		
	α-Amy IC_{50}, μg mL^{-1}	α–Glu IC_{50}, μg mL^{-1}	$O_2^{\bullet-}$ IC_{50}, μg mL^{-1}	HClO IC_{50}, μg mL^{-1}	$ROO^{\bullet}$ μmol TE mg^{-1} DW
OHS-E	7.73 ± 0.84[a]	49.44 ± 1.53[b]	43.08 ± 1.11[a]	43.08 ± 1.11[a]	2.16 ± 0.28[b]
Acarbose	9.28 ± 0.55[a]	74.91 ± 1.24[a]			
Gallic acid			10.39 ± 1.60[c]	5.51 ± 0.34[a]	7.51 ± 0.40[b]
Catechin			26.24 ± 0.15[b]	0.32 ± 0.02[b]	237.11 ± 28.37[a]

Results are reported as the mean ± SD ($n = 4$). TE stands for Trolox equivalents. Different lowercase letters in the same column indicate significant differences (Tukey's test, $p < 0.05$).

LC-MS profiling of OHS-E/identification and quantification of bioactive compounds in OHS-E

The phytochemical profile of OHS-E was successfully obtained by HPLC/ESI-MS/MS analysis in negative ionization mode (Fig. 2). All putatively identified and quantified compounds are listed in Table 4. A thorough analysis of molecular masses, characteristic fragmentation patterns, along with the chemical structures (Supporting information, Fig. S2), are provided in the Supporting information (section 2).

Notably, 47 compounds were tentatively identified, with a higher abundance of lipids (24 compounds) and polyphenols (15 compounds), followed by organic acids (seven compounds). Considering lipids, 12 hydroxy fatty acids (**24**–**29, 31, 33, 34, 36, 38** and **43**) and six unsaturated fatty acids (**32, 35, 37, 39, 40** and **45**) were identified. A glycerophospholipid (**18**), branched (**41** and **46**) and straight chain (**42, 44** and **47**) fatty acids were also annotated. Nevertheless, (C18:0) dihydroxy stearic acid (**38**) constituted the most intense peak of the TIC chromatogram (Fig. 2). (C18:1) Trihydroxy-octadecenoic acid isomers (**27** and **28**) and (C16:0; O2) dihydroxy-hexadecanoic acid isomer (**29**) were previously detected by Masullo *et al.*[13] in hazelnut shells as the only constituents of the fatty acids class. Moreover, compounds **27** and **28** have been reported as the most abundant ones in a hydro-alcoholic walnut shell extract obtained by MAE.[7]

Among polyphenols, lignans (**5**, **12**, **16**, **19** and **23**), flavonoids (**13**, **14**, **17** and **30**), a stilbene (**10**), an hydroxycoumarin (**11**) and cyclic diarylheptanoids (**6**, **7**, **20** and **22**) were identified in OHS-E. Lignans **5**, **16**, **19** and **23** were identified herein for the first time in hazelnut shells. Diarylheptanoids were named 'giffonins' by Masullo *et al.*[13] that previously isolated them from *C. avellana* leaves, male flowers, shells and green leafy involucres extracted with ethanol, providing a first evidence of the inhibitory activity of these compounds towards α-glucosidase. Lastly, valuable organic acids were annotated in the extract, mainly gallic acid (**4**) and two gallic acid derivatives (**15** and **21**), shikimic acid (**8**) and ellagic acid (**11**).

The areas of non-overlapping signals in the mass chromatogram were considered to provide quantitative information as described in the Materials and methods. Gallic acid, quercetin-3-*O*-glucoside and C18:1 linoleic acid were employed as standards for the quantification of constituents related to them. Thus, compounds **8**,**15** and **21** were quantified as gallic acid, **30** was quantified with quercetin-3-*O*-glucoside, and **25, 31–34, 36, 38–42, 46** and **47** were quantified with C18:2 linoleic acid. Coeluting compounds (**32** and **33**) were quantified together.

Overall, OHS-E prepared by MAE was rich in lipids and phenolic compounds, for which the abundance originates from the combined polarities of the water/ethanol solvent system employed in this study, as previously found for other dry fruit shells extracted with this same solvent mixture.[7,8,26] Furthermore, these results highlighted MAE as a versatile technique for extracting a wide range of compounds at shorter times compared to conventional methods.

 © 2024 The Author(s).
Journal of the Science of Food and Agriculture published by John Wiley & Sons Ltd on behalf of Society of Chemical Industry.

ROS scavenging capacity of OHS-E

Phenolic compounds are considered nutraceuticals due to their potential efficacy in offsetting ROS overproduction in oxidative stress-related diseases, such as T2DM.[1] In this context, for the first time, an extract from hazelnut shells was tested as potential antiradical agent towards ROO$^{\bullet}$, HClO and $O_2^{\bullet-}$ (Table 5). OHS-E exhibited a high ability to quench ROO$^{\bullet}$ (2.16 μmol TE mg^{-1} DW), being not significantly ($p > 0.05$) different from gallic acid (positive control; 7.51 μmol TE mg^{-1} DW), which was used as positive control. Moreover, this result was substantially higher than the one reported by Maccarronello *et al.* (0.72 μmol TE mg^{-1} DW) for *Pistacia vera* L. shells extracted by MAE.

Considering that the lower the IC_{50}, the higher the antiradical capacity, results (Table 5) indicated that even HClO was effectively scavenged by OHS-E (IC_{50} = 11.04 μg mL^{-1}). Even if gallic acid (IC_{50} = 5.51 μg mL^{-1}) and catechin (IC_{50} = 0.32 μg mL^{-1}) showed a higher HClO-scavenging capacity, a lower result (IC_{50} = 17.23 μg mL^{-1}) was reported for an ethanolic *Castanea sativa* shell extract prepared by MAE at comparable ethanol concentration.[27] Nevertheless, HClO scavenging capacity of OHS-E was lower than that exhibited by a hydroalcoholic extract (IC_{50} = 4.70 μg mL^{-1}) of *P. vera* L. shells.[8]

Concerning $O_2^{\bullet-}$, OHS-E showed an IC_{50} of 43.08 μg mL^{-1}, suggesting a lower antiradical capacity compared to catechin (IC_{50} = 26.24 μg mL^{-1}) and gallic acid (IC_{50} = 10.39 μg mL^{-1}). Moreover, OHS-E showed a minor scavenging efficiency towards $O_2^{\bullet-}$ compared to *C. sativa* shells extract obtained by MAE with 25% of ethanol in water concentration (IC_{50} = 29.15 μg mL^{-1}).[27] Nevertheless, OHS-E showed a higher $O_2^{\bullet-}$ quenching capacity than the one reported for *P. vera* L. shells (IC_{50} = 54.92 μg mL^{-1}) extracted by MAE.[8]

ROS scavenging efficiency of OHS-E could be explained by its phytochemical constituents, particularly by the presence of ellagic acid, isofraxidin, gallic acid derivatives, as well as cyclic diarylheptanoids (giffonins), for which antioxidant/antiradical activities have been previously reported.[6,11,28,29]

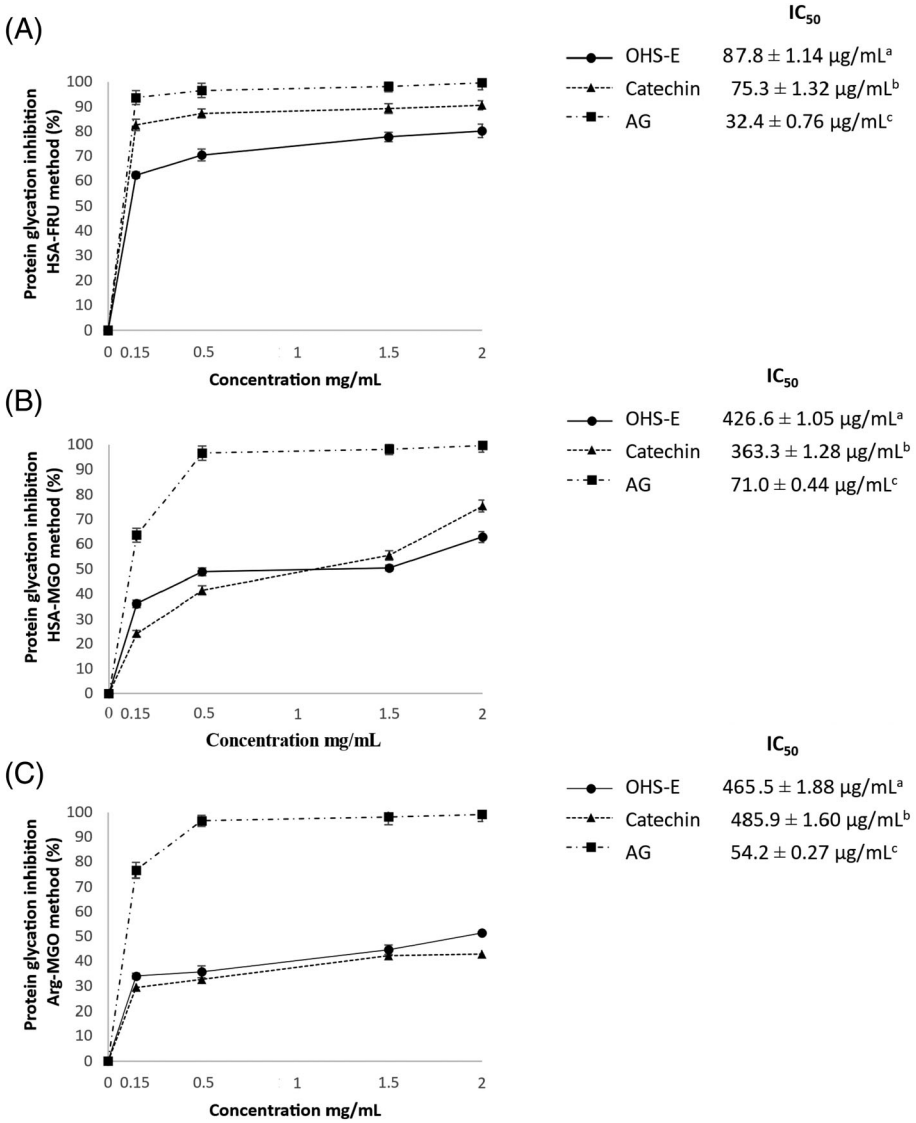


Figure 3. AGE inhibitory effect of OHS-E using (a) human serum albumin-fructose (HSA-FRU), (b) HSA-methylglyoxal (HSA-MGO) and (c) arginine-methylglyoxal (Arg-MGO) reaction systems, respectively. Aminoguanidine (AG) and catechin were used as positive controls. Results (mean ± SD) were expressed as a percentage of fluorescent AGE inhibition (%) and as half maximal inhibitory concentration (IC_{50}) values. Different letters indicate a significant difference ($p < 0.05$, Tukey's test).

 © 2024 The Author(s).
Journal of the Science of Food and Agriculture published by John Wiley & Sons Ltd on behalf of Society of Chemical Industry.

Hypoglycaemic activity of OHS-E

Herein, the inhibitory activity of *C. avellana* shells towards α-amylase was for the first time investigated. As shown in Table 5, OHS-E exhibited an inhibitory effect (IC_{50} = 7.73 μg mL^{-1}) comparable to the anti-diabetic drug acarbose (IC_{50} = 9.28 μg mL^{-1}). However, OHS-E inhibitory effect towards α-amylase was lower than the one (IC_{50} = 2.05 μg mL^{-1}) reported for *P. vera* shell extract.[8] Concerning α-glucosidase inhibitory activity (Table 5), OHS-E showed an IC_{50} of 49.44 μg mL^{-1}, suggesting a higher hypoglycaemic effect when compared to acarbose (IC_{50} = 74.91 μg mL^{-1}). This result was in line with the one obtained for *P. vera* shells (IC_{50} = 41.07 μg mL^{-1}) extracted by MAE.[8]

Overall, these results highlighted the promising potential of OHS-E to be employed as α-amylase and α-glucosidase inhibitor in hypoglycemic preparations. Fatty acids, such as (C18:2)-linoleic acid (**39**), as well as cyclic diarylheptanoids, namely giffonin P (**7**), giffonin U (**8**), carpinontriol B (**21**) and giffonin V (**23**), as detected in the phytochemical profile of OHS-E, could explain such notable inhibitory activity. Masullo *et al.*[13] assessed the α-glucosidase inhibitory activity of diarylheptanoids isolated from *C. avellana* 'Tonda di Giffoni' by-products, reporting giffonins as the most active inhibitors. Other studies have also reported the hypoglycaemic effect of fatty acids.[30-32]

Anti-glycation effects of OHS-E

In the present study, HSA-fructose (HSA-FRU), HSA-methylglyoxal (HSA-MGO) and arginine-methylglyoxal (Arg-MGO) reaction systems were adopted to investigate, for the first time, the anti-glycation effects of phytochemicals from *C. avellana* L. shells. Figure 3 compares fluorescent AGE inhibition percentages (%) and the IC_{50} values of OHS-E with those of catechin, which inhibition efficiency towards AGE formation has been previously reported.[2,33] In all systems, AG showed the highest anti-glycation activity, whereas OHS-E inhibited fluorescent AGE formation in a dose-dependent manner. Notably, in the HSA-FRU model (Fig. 3a), OHS-E scavenged over 62.4% of AGEs at the lowest tested concentration (0.15 mg mL^{-1}), reaching a maximum of 80.2% at 2 mg mL^{-1}, with an IC_{50} of 87.8 μg mL^{-1}. Although AGE inhibitory efficiency of catechin was superior to OHS-E, our extract was more effective than the hazelnut skin extract (IC_{50} = 109.70 μg mL^{-1}) obtained by UAE[34] and *Plinia cauliflora* peel extract (IC_{50} = 230 μg mL^{-1}).[35] Concerning HSA-MGO system (Fig. 3b), OHS-E resulted in a weaker methylglyoxal scavenger (IC_{50} = 426.6 μg mL^{-1}) when compared to catechin (IC_{50} = 363.3 μg mL^{-1}). However, *Camellia oleifera* shells showed a lower anti-AGEs capacity (IC_{50} = 641.86 μg mL^{-1}) than OHS-E in the HSA-MGO method.[36] Interestingly, in the Arg-MGO system (Fig. 3c), the inhibitory effect of OHS-E (IC_{50} = 465.5 μg mL^{-1}) was significantly ($P < 0.05$) stronger than catechin (IC_{50} = 485.9 μg mL^{-1}), suggesting a greater ability of OHS-E in preventing the methylglyoxal-induced formation of the fluorescent AGE argpyrimidine.[2]

Altogether, these results indicated the ability of OHS-E to counteract AGE formation in all steps of the glycation cascade. Such an effect could mainly depend on the phenolic acids identified in the extract, including shikimic and ellagic acid, for which anti-glycation activity has been reported in previous studies.[37,38]

Effect of OHS-E towards Caco-2 and HT29-MTX

Given its potential antioxidant and anti-diabetic effects, exploring the biocompatibility of OHS-E with human colon epithelial cells (Caco-2 and HT29-MTX) offered valuable preliminary data before advancing to *in vivo* studies. As shown in Fig. 4, OHS-E exhibited an intestinal cell viability exceeding 72.9% at all tested concentrations (62.5–1000 mg mL^{-1}). Specifically, the extract did not significantly ($p > 0.05$) affect HT29-MTX viability, which was higher than 79.7% (Fig. 4). Regarding Caco-2, the viability was higher than 83.3% at concentrations ranging from 62.5 to 250 μg mL^{-1}, whereas a significant ($p > 0.05$) decrease was observed at higher OHS-E concentrations (500 and 1000 μg mL^{-1}) (Fig. 4). Accordingly, the optimal not cytotoxic concentrations were ≤ 1000 and ≤ 250 μg mL^{-1} for HT29-MTX and Caco-2 cells, respectively. The greater sensitivity of Caco-2 compared to HT29-MTX has already noted in previous studies.[8,39] Furthermore, these results were similar to those reported by Maccarronello *et al.*[8] who exposed Caco-2 and HT29-MTX to different concentrations (62.5–1000 μg mL^{-1}) of an hydroalcoholic extract from *P. vera* L. shells, observing an intestinal cell viability higher than 75.93%. Conversely, the exposure of both cell lines to the highest tested concentration (1000 μg mL^{-1}) of a *C. sativa* shells extract obtained by subcritical water extraction led to cell viabilities of 9.06% and 6.29% for Caco-2 and HT29-MTX, respectively.[16] As far as we know, this was the first study to report the influence of phytochemicals recovered from hazelnut shells on Caco-2 and HT29-MTX intestinal cells.

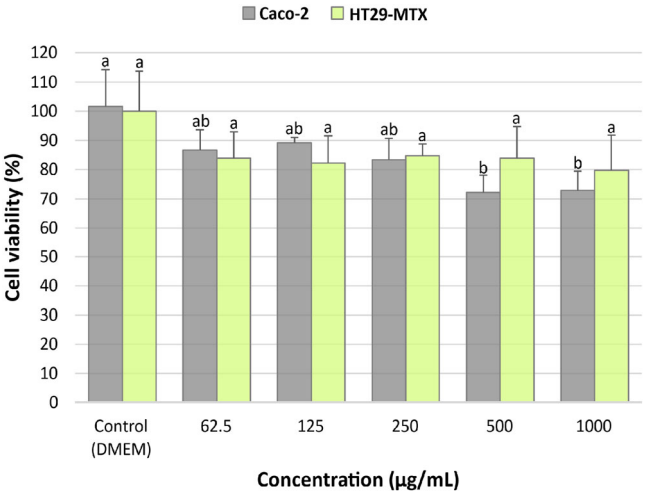


Figure 4. Effects of OHS-E on the viability of Caco-2 and HT29-MTX cell lines at a concentration range between 62.5 and 1000 μg mL^{-1}. OHS-E was assayed in quadruplicate and results are reported as the mean ± SD of two independent experiments. Different letters (a, b) indicate significant differences (Tukey's test, $p < 0.05$) compared to the control.

CONCLUSIONS

The present study provides results that promote the valorization of *C. avellana* L. shells extracted by a completely eco-sustainable approach (MAE). OHS-E obtained under optimal conditions (28% *v/v* ethanol/water, 270 *s*, 670 *W* and 37 mL g^{-1}), showed the utmost TPC and antioxidant/antiradical efficiencies, with no significant ($p < 0.05$) difference with the predicted values, supporting the reliability of the developed BBD model. LC-MS analysis highlighted a high recovery of a variety of lipids and phenolic compounds, which could explain the strong inhibition capacity of OHS-E towards ROS and carbohydrate hydrolysing enzymes (α-amylase and

 © 2024 The Author(s).
Journal of the Science of Food and Agriculture published by John Wiley & Sons Ltd on behalf of Society of Chemical Industry.

α-glucosidase). Furthermore, the anti-glycation effects of phytochemicals from *C. avellana* shells were reported for the first time. Biocompatibility studies on intestinal cells revealed a slight reduction in Caco-2 viability at OHS-E doses above 250 μg mL^{-1} (72.9%), whereas HT29-MTX viability was not significantly affected at all tested concentrations.

As a result of the complex composition of OHS-E, future studies should use isolated compounds to discover the main contributors to the bioactivities studied here. These findings demonstrate that OHS-E could effectively represent a promising ingredient for developing an anti-diabetic oral nutraceutical formulation. Further 3D intestinal permeability models and *in vivo* studies are requested to fully validate this new application, evaluating the effects of the digestive environment on the antiradical and hypoglycaemic properties of OHS-E and gaining information on the stability of its active constituents.

AUTHOR CONTRIBUTIONS

AEM and NC were responsible for methodology. AEM and ADF were responsible for validation. AEM was responsible for formal analysis. AEM, AMS, ADF, PCC and FR were responsible for investigation. AEM was responsible for writing the original draft. NC, PCC, FR and VM were responsible for reviewing and editing. NC, AMS, FR and VM were responsible for visualization. NC, FR and VM were responsible for supervision. FR and VM were responsible for resources. FR and VM were responsible for funding acquisition. VM was responsible for project administration and conceptualization.

ACKNOWLEDGEMENTS

We gratefully acknowledge the Bio-Nanotech Research and Innovation Tower of the University of Catania (BRIT; project PONa3_00136), financed by the Italian Ministry for University and Research (MUR), for the availability of the Synergy H1 microplate reader. Anna Elisabetta Maccarronello is grateful for the PhD grant (D.M. n 1061, PON R&I 2014/2020, 2020/2021 – Cycle 37) financed by the Italian Ministry for Education, University and Research MIUR. Ana Margarida Silva is grateful for the PhD grant (SFRH/BD/144994/2019) financed by POPH-QREN and subsidized by the European Science Foundation and Ministério da Ciência, Tecnologia e Ensino Superior. Francisca Rodrigues (2023.06819.CEECIND) is grateful for her contract financed by FCT/MCTES—CEEC Individual Program Contract. Open access publishing facilitated by Universita degli Studi di Catania, as part of the Wiley - CRUI-CARE agreement.

FUNDING INFORMATION

This work was financed by MUR ITALY PRIN 2022 PNRR (Project No. P2022MWY3P) and by national funds from FCT – Fundação para a Ciência e a Tecnologia, I.P., in the scope of the project UIDP/04378/2020 and UIDB/04378/2020 of the Research Unit on Applied Molecular Biosciences – UCIBIO and the project LA/P/0140/2020 of the Associate Laboratory Institute for Health and Bioeconomy – i4HB.

CONFLICT OF INTEREST

The authors declare that they have no conflicts of interest.

DATA AVAILABILITY STATEMENT

The data that support the findings of this study are available from the corresponding author upon reasonable request.

SUPPORTING INFORMATION

Supporting information may be found in the online version of this article.

REFERENCES

1 Ullah A, Khan A and Khan I, Diabetes mellitus and oxidative stress-a concise review. *Saudi Pharm J* **24**:547–553 (2016).
2 Wang W, Yagiz Y, Buran TJ, Nunes CD and Gu LW, Phytochemicals from berries and grapes inhibited the formation of advanced glycation end-products by scavenging reactive carbonyls. *Food Res Int* **44**: 2666–2673 (2011).
3 Anis MA and Sreerama YN, Inhibition of protein glycoxidation and advanced glycation end-product formation by barnyard millet (*Echinochloa frumentacea*) phenolics. *Food Chem* **315**:126265 (2020).
4 Tundis R, Loizzo MR and Menichini F, Natural products as α-amylase and α-glucosidase inhibitors and their hypoglycaemic potential in the treatment of diabetes: an update. *Mini Rev Med Chem* **10**:315–331 (2010).
5 Chinchansure AA, Korwar AM, Kulkarni MJ and Joshi SP, Recent development of plant products with anti-glycation activity: a review. *RSC Adv* **5**:31113–31138 (2015).
6 Pinto D, Cadiz-Gurrea MD, Sut S, Ferreira AS, Leyva-Jimenez FJ, Dall'Acqua S *et al.*, Valorisation of underexploited *Castanea sativa* shells bioactive compounds recovered by supercritical fluid extraction with CO_2: a response surface methodology approach. *J CO2 Util* **40**:101194 (2020).
7 Muccilli V, Maccarronello AE, Rasoanandrasana C, Cardullo N, de Luna MS, Pittalà MGG *et al.*, *Green^3: A Green Extraction of Green Additives for Green Plastics*. SSRN, Heliyon (2024).
8 Maccarronello AE, Cardullo N, Silva AM, Di Francesco A, Costa PC, Rodrigues F *et al.*, From waste to bioactive compounds: a response surface methodology approach to extract antioxidants from *Pistacia vera* shells for postprandial hyperglycaemia management. *Food Chem* **443**:138504 (2024).
9 Di Nunzio M, Hazelnuts as source of bioactive compounds and health value underestimated food. *Curr Res Nutr Food Sci* **7**:17–28 (2019).
10 Allegrini A, Salvaneschi P, Schirone B, Cianfaglione K and Di Michele A, Multipurpose plant species and circular economy: *Corylus avellana* L. as a study case. *Front Biosci-Landmark* **27**:011 (2022).
11 Masullo M, Cerulli A, Mari A, Santos CCD, Pizz C and Piacente S, LC-MS profiling highlights hazelnut (Nocciola di Giffoni PGI) shells as a byproduct rich in antioxidant phenolics. *Food Res Int* **101**:180–187 (2017).
12 Yuanu B, Lu M, Eskridge KM and Hanna MA, Valorization of hazelnut shells into natural antioxidants by ultrasound-assisted extraction: process optimization and phenolic composition identification. *J Food Process Eng* **41**:e12692 (2018).
13 Masullo M, Lauro G, Cerulli A, Bifulco G and Piacente S, *Corylus avellana*: a source of diarylheptanoids with α-glucosidase inhibitory activity evaluated by *in vitro* and *in silico* studies. *Front Plant Sci* **13**:805660 (2022).
14 Di Michele A, Pagano C, Allegrini A, Blasi F, Cossignani L, Raimo ED *et al.*, Hazelnut shells as source of active ingredients: extracts preparation and characterization. *Molecules* **26**:6607 (2021).
15 Yuan B, Lu M, Eskridge KM, Isom LD and Hanna MA, Extraction, identification, and quantification of antioxidant phenolics from hazelnut (*Corylus avellana* L.) shells. *Food Chem* **244**:7–15 (2018).
16 Pinto D, Vieira EF, Peixoto AF, Freire C, Freitas V, Costa P *et al.*, Optimizing the extraction of phenolic antioxidants from chestnut shells by subcritical water extraction using response surface methodology. *Food Chem* **334**:127521 (2021).
17 Cardullo N, Leanza M, Muccilli V and Tringali C, Valorization of agri-food waste from pistachio hard shells: extraction of polyphenols as natural antioxidants. *Resources* **10**:45 (2021).
18 Di Stefano V, Buzzanca C, Ruvutuso F, Scuderi D, Palazzolo E, Gugliuzza G *et al.*, Chemical composition and anti-radical properties

 © 2024 The Author(s).
Journal of the Science of Food and Agriculture published by John Wiley & Sons Ltd on behalf of Society of Chemical Industry.

of coffee cherry cultivated in Mediterranean climate. *Food Biosci* **56**: 103349 (2023).
19 Gomes A, Fernandes E, Silva AMS, Santos CMM, Pinto D, Cavaleiro JAS *et al*., 2-Styrylchromones: novel strong scavengers of reactive oxygen and nitrogen species. *Bioorg Med Chem* **15**:6027–6036 (2007).
20 Cardullo N, Floresta G, Rescifina A, Muccilli V and Tringali C, Synthesis and in vitro evaluation of chlorogenic acid amides as potential hypoglycemic agents and their synergistic effect with acarbose. *Bioorg Chem* **117**:105458 (2021).
21 Dahmoune F, Nayak B, Moussi K, Remini H and Madani K, Optimization of microwave-assisted extraction of polyphenols from Myrtus communis L. leaves. *Food Chem* **166**:585–595 (2015).
22 Picot-Allain C, Mahomoodally MF, Ak G and Zengin G, Conventional versus green extraction techniques - a comparative perspective. *Curr Opin Food Sci* **40**:144–156 (2021).
23 Nayak B, Dahmoune F, Moussi K, Remini H, Dairi S, Aoun O *et al*., Comparison of microwave, ultrasound and accelerated-assisted solvent extraction for recovery of polyphenols from Citrus sinensis peels. *Food Chem* **187**:507–516 (2015).
24 Lopez-Salazar H, Camacho-Diaz BH, Ocampo MLA and Jimenez-Aparicio AR, Microwave-assisted extraction of functional compounds from plants: a review. *Bioresources* **18**:6614–6638 (2023).
25 Mohammad NA, Zaidel DNA, Muhamad II, Hamid MA, Yaakob H and Jusoh YMM, Optimization of the antioxidant-rich xanthone extract from mangosteen (*Garcinia mangostana* L.) pericarp via microwave-assisted extraction. *Heliyon* **5**:e02571 (2019).
26 Razola-Diaz MD, Gomez-Caravaca AM, Guerra-Hernandez EJ, Garcia-Villanova B and Verardo V, New advances in the phenolic composition of tiger nut (*Cyperus esculentus* L.) by-products. *Foods* **11**:343 (2022).
27 Pinto D, Silva AM, Freitas V, Vallverdú-Queralt A, Delerue-Matos C and Rodrigues F, Microwave-assisted extraction as a green technology approach to recover polyphenols from *Castanea sativa* shells. *ACS Food Sci Technol* **1**:229–241 (2021).
28 Li P, Zhao QL, Wu LH, Jawaid P, Jiao YF, Kadowaki M *et al*., Isofraxidin, a potent reactive oxygen species (ROS) scavenger, protects human leukemia cells from radiation-induced apoptosis via ROS/mitochondria pathway in p53-independent manner. *Apoptosis* **19**:1043–1053 (2014).
29 Richard D, Kefi K, Barbe U, Bausero P and Visioli F, Polyunsaturated fatty acids as antioxidants. *Pharmacol Res* **57**:451–455 (2008).
30 Nguyen TH and Kim SM, α-glucosidase inhibitory activities of fatty acids purified from the internal organ of sea cucumber *Stichopus japonicas*. *J Food Sci* **80**:H841–H847 (2015).
31 Teng H and Chen L, α-Glucosidase and α-amylase inhibitors from seed oil: a review of liposoluble substance to treat diabetes. *Crit Rev Food Sci Nutr* **57**:3438–3448 (2017).
32 Su CH, Hsu CH and Ng LT, Inhibitory potential of fatty acids on key enzymes related to type 2 diabetes. *Biofactors* **39**:415–421 (2013).
33 Wu Q, Tang SM, Zhang L, Xiao JS, Luo Q, Chen YY *et al*., The inhibitory effect of the catechin structure on advanced glycation end product formation in alcoholic media. *Food Funct* **11**:5396–5408 (2020).
34 Spagnuolo L, Della Posta S, Fanali C, Dugo L and De Gara L, Antioxidant and antiglycation effects of polyphenol compounds extracted from hazelnut skin on advanced glycation end-products (AGEs) formation. *Antioxidants* **10**:424 (2021).
35 Borges LLR, de Oliveira LL, Freitas VV, Leite BRD, Nascimento A, Castro GAD *et al*., Digestive enzymes inhibition, antioxidant and antiglycation activities of phenolic compounds from jabuticaba (*Plinia cauliflora*) peel. Food. *Bioscience* **50**:102195 (2022).
36 Peng JM, Wen WJ, Liang GQ, Huang WY, Qiu ZH, Wang Q *et al*., *Camellia oleifera* shells polyphenols inhibit advanced glycation end-products (AGEs) formation and AGEs-induced inflammatory response in RAW264.7 macrophages. *Ind Crops Prod* **197**:116589 (2023).
37 Al-Malki AL, Shikimic acid from *Artemisia absinthium* inhibits protein glycation in diabetic rats. *Int J Biol Macromol* **122**:1212–1216 (2019).
38 Kumagai Y, Nakatani S, Onodera H, Nagatomo A, Nishida N, Matsuura Y *et al*., Anti-glycation effects of pomegranate (*Punica granatum* L.) fruit extract and its components in vivo and in vitro. *J Agric Food Chem* **63**:7760–7764 (2015).
39 Pinto D, Franco SD, Silva AM, Cupara S, Koskovac M, Kojicic K *et al*., Chemical characterization and bioactive properties of a coffee-like beverage prepared from *Quercus cerris* kernels. *Food Funct* **10**: 2050–2060 (2019).

 © 2024 The Author(s).
Journal of the Science of Food and Agriculture published by John Wiley & Sons Ltd on behalf of Society of Chemical Industry.